Formation of graphene and hexagonal boron nitride on Rh(111) studied by in-situ scanning tunneling microscopy

Dong, G.

Chapter 4 Nanomesh formation at different temperatures on Rh(111)

4.1 Introduction

The procedure, originally introduced by Corso *et al.* for the formation of a nanomesh film, is to expose the Rh(111) surface to borazine $(HBNH)_3$ gas at 1050 K [6]. The temperature seems to be an important parameter, as mentioned in section 3.1. In order to investigate the influence of the temperature on the formation of the *h*-BN nanomesh structure, borazine $(HBNH)_3$ was deposited at various temperatures onto Rh(111). In addition to this, we also investigated the evolution of the overlayer with temperature after the deposition by heating the sample to higher temperatures while imaging the surface continuously by STM.

4.2 Nanomesh formation from borazine deposited at room temperature

We first exposed a cleaned Rh(111) surface to 4 x 10^{-5} mbar s of borazine at room temperature. This pre-exposed surface was heated up slowly, from room temperature to ~1060 K, while STM images were taken continuously. Selected images from this measurement are shown in Fig. 4.1A complete STM-movie, from 295 to 1057 K, is available online [79]. At 690 K, the first noticeable rearrangements into small, nanometer-scale clusters were observed. As the temperature increased further, these small clusters became mobile, and coalesced. The branched and elongated shapes, observed in Fig. 4.1B, are characteristic of a diffusion-limited type of aggregation (DLA)

[80]. Within the individual clusters, distinct height variations were seen, with a typical amplitude of 0.05 nm (Fig. 4.1B). This indicates that these were not mere clusters of borazine molecules, but that instead, the clusters already had the *h*-BN structure, with a thickness of a single monolayer and with the corrugation resulting from the mismatch with the underlying Rh lattice. In Fig. 4.1C, it can be seen that, at a high temperature of 1007 K, the shapes of the islands had become more compact, and the height variations had organized into the nanomesh superstructure, albeit with a high density of defects. When the temperature was further increased to 1042 K, most of these defects disappeared, and the islands ripened to larger sizes (Fig. 4.1D). The images in Fig. 4.1B-D clearly show that the total coverage was well below that corresponding to a full *h*-BN nanomesh monolayer, even though the initial exposure of 40 L had been sufficient to reach the maximum coverage at room temperature. What these images also indicate is that there was, at most, a minor loss of material (borazine or BN) from the surface. This implies that almost all the B- and N-atoms deposited at room temperature were still present at 1042 K, and that their numbers added up to no more than a 50% monolayer of *h*-BN. Two potential causes for this lack of material are (i) that, at room temperature, the borazine molecules formed a highly disordered, and therefore, non-compact layer (Fig. 4.1A), and (ii), that with most of their hydrogen atoms still present, the borazine molecules, initially present at room temperature, required more space than that occupied their B- and N-atoms, after hydrogen desorption, in the final *h*-BN structure. From this first experiment, we conclude that the typical deposition temperature of 1050 K is not necessary for borazine adsorption or *h*-BN formation. Furthermore, it was observed that the overlayer was formed via two-dimensional nucleation and growth.

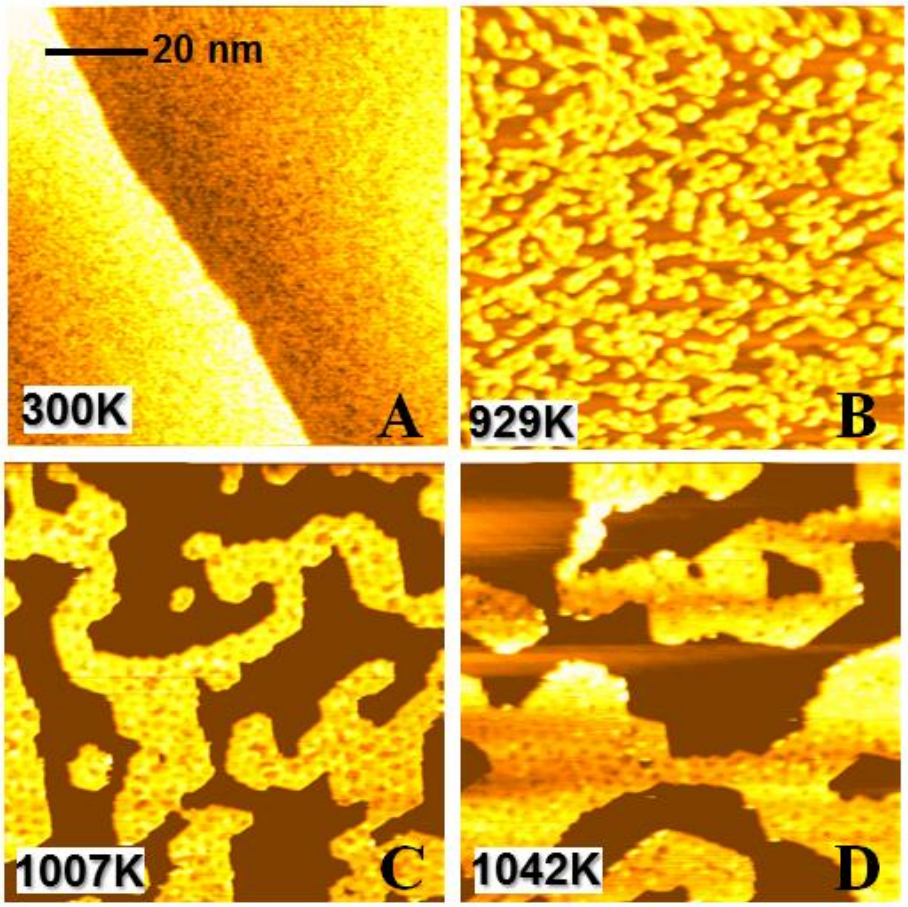

Fig. 4.1 A series of images selected from the STM Movie 1 [79], during a continuous temperature ramp from 300 K to 1057 K of a borazine-pre-exposed Rh(111) surface. (A) The Rh surface directly after exposure to 40 L of borazine gas at room temperature. A monatomic step on the Rh surface crosses the image. The rough appearance of the upper and lower terraces is caused by the borazine deposit. (B) At higher temperatures, the overlayer first organized into narrow, somewhat elongated islands of *h*-BN. The height variations within the islands result from the mismatch between the lattice constants of the overlayer and the substrate. (C) The next stage was the formation of more compact *h*-BN islands, with a defective nanomesh superstructure. (D) At the final temperature, the nanomesh structure was relatively well-defined.
All images are 85 nm × 85 nm, and have been taken at a sample voltage of $V_b = 3.0$ V and a tunneling current of $I_t = 0.05$ nA.

4.3 Nanomesh formation from borazine deposited between 627 K and 865 K

As suggested by the fractal-like island growth patterns in Fig. 4.1B, after pre-exposure of the Rh substrate to borazine at room temperature, the initial *h*-BN islands are formed by diffusion-limited aggregation [80] of individual borazine molecules or small borazine clusters. Next, we address the role of the substrate temperature during the exposure. For this, we exposed the substrate to borazine at 627 K. After 10 minutes at a pressure of 3.7×10^{-10} mbar, the STM images showed no sign of either borazine adsorption or *h*-BN formation. A significantly higher pressure of 1.5×10^{-9} mbar was required to obtain the first stages of island formation; Fig. 4.2A shows an example at a somewhat higher pressure of 3.2×10^{-9} mbar. While the terraces exhibited a low density of nuclei, the steps on the Rh substrate were saturated by small islands. The shapes of these islands were again fractal-like. No corrugation was observed on the islands, which means that they did not yet have the structure of *h*-BN. Then we increased the sample temperature. Whereas at 762 K the islands still retained their fractal shapes, at 806 K they had become compact (Fig. 4.2B). In addition, as we will discuss in more detail in secton 5.1, the orientations of the island edges indicate that in this temperature window the island rearrangements had involved the breaking of B-N bonds. Fig. 4.2B further illustrates that at 806 K the *h*-BN islands did not merely occur at steps of the Rh substrate. The islands displayed a variety of orientations, the preferred orientation being the one with the *h*-BN lattice, and therefore also the moiré pattern, aligned with the Rh(111) substrate.

On this *h*-BN seeded surface, with different orientations, further *h*-BN was formed by exposing the surface to borazine pressures ranging from 1.2×10^{-9} to 1.2×10^{-8} mbar, while the substrate temperature was held at 865 K. Fig. 4.2C and D show the same area before and after this extra deposition. They show that most of the additional *h*-BN closely followed the orientations of the ‘seed’ islands. At every location where two domains met, a domain boundary line or a defect line was formed between them. However, there were exceptions. For example, the domain indicated by the black arrow in Fig. 4.2D was newly formed at the connection between two differently oriented domains, suggesting that the mismatch between these orientations was so unfavorable, that in spite of the extra domain boundary length, the new domain could lower the total energy. Further evidence

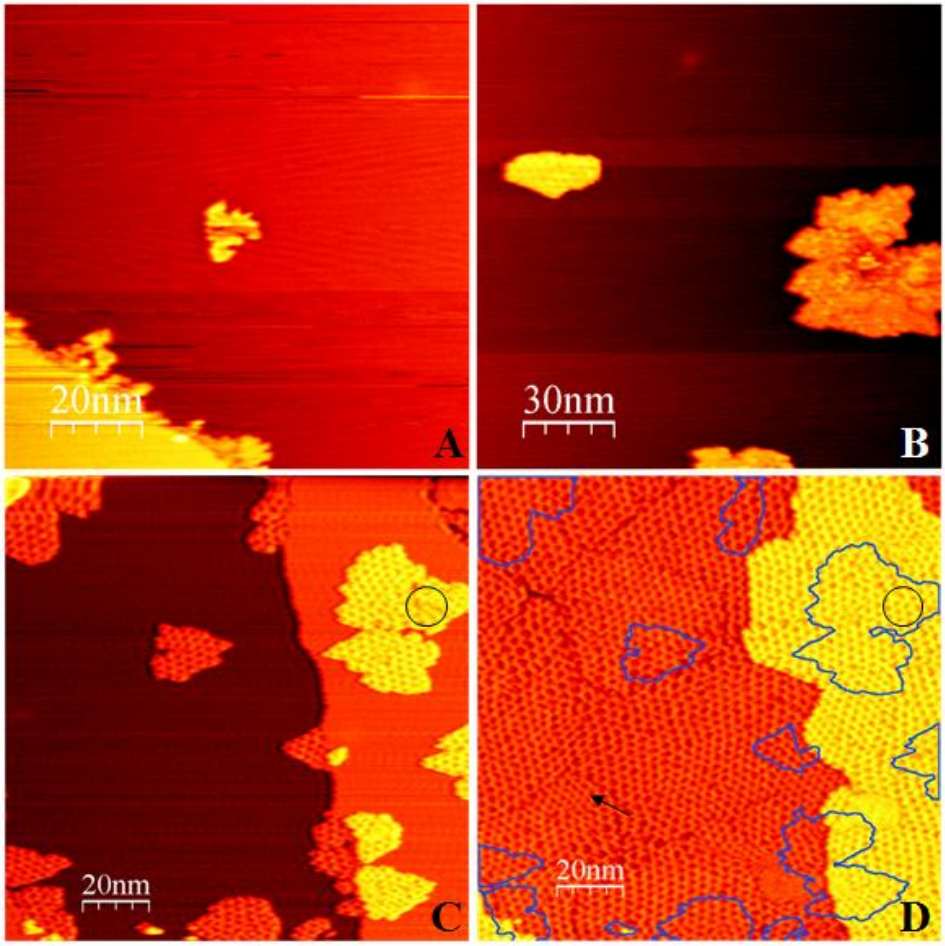

Fig. 4.2 (A) STM image of Rh(111) at 627 K, after having been exposed at that temperature to 3 x 10^{-9} mbar of borazine for 12 minutes. The Rh steps were saturated by small islands and the shapes of islands were fractal-like. (B) STM image after the temperature had been increased to 806 K. The *h*-BN islands appeared to be compact. Within each island, the nanomesh superstructure can be observed. The islands did not occur primarily at steps of the Rh substrate. (C) After a further temperature increase to 865 K, the islands had become more compact. (D) The same area as in panel C, after an additional borazine exposure at pressures ranging from 2 x 10^{-9} to 1.2 x 10^{-8} mbar for 78 minutes, while the temperature of the sample was held at 865 K. The surface was fully covered by *h*-BN with a variety of orientations. The blue lines indicate the contours of the initial islands in panel C. Most of the growth followed the orientations of these initial islands. The black arrow indicates a new domain that had formed during growth. In the circled part, defects had been removed that were still present in panel C.
V_b = 2.9, 2.8 V, -1.0 V, -1.0V for panels A – D, respectively, I_t = 0.05 nA.

were present in the initial islands. For example, the defect marked by a circle in Fig. 4.2C was no longer present in Fig. 4.2D. Similar effects can be seen in Fig. 4.1. But the removal of defects occurred far less frequently than the formation of defect lines where different domains encountered one another. As a result, the completed *h*-BN overlayer contained a significant density of defects. A detailed discussion of these defects will be given in Chapter 6.

4.4 Nanomesh formation from borazine deposited at 978 K

In section 4.2 we concluded that the typical deposition temperature of 1050 K of *h*-BN on Rh(111) is not necessary for borazine adsorption or for *h*-BN formation. Furthermore, we saw that the overlayer formed via two-dimensional nucleation and growth. Due to the procedure adopted in section 4.2, where the borazine was deposited at room temperature and the substrate was subsequently heated, the resulting structure was far from a perfectly regular nanomesh. In order to find out what really limits the quality of growing nanomesh films, it was necessary to perform STM observations *during* borazine exposure close to the reported optimal nanomesh formation conditions (e.g. 1050 K [6]). Exposing a clean Rh(111) surface to borazine at 978 K, we verified that, also at such a high temperature, the overlayer assembled via the two-dimensional nucleation-and-growth mode, in this case, with compact and well-separated *h*-BN islands that immediately adopted a regular nanomesh structure. However, under these conditions, the average density of the islands was so low, e.g. 3 islands/μm^2, that it was difficult to capture the interesting stages of the process in well-resolved STM images. Therefore, the nucleation density was artificially increased by a seeding procedure, which consisted of first exposing the Rh surface to a low dose of 0.2 L borazine at room temperature, followed by a heating step to 978 K, which resulted in the formation of a comfortable density of 250 islands/μm^2 of small *h*-BN islands (Fig. 4.3A). On this seeded surface, we continued the borazine exposure at 978 K, while imaging continuously by STM.

4.4.1 The growth unit

The first thing that was noticed was that the growth appeared to proceed by the addition of entire nanomesh units, or by rows of nanomesh units. This discretization of the growth process in nanomesh units is illustrated by Fig. 4.3B and C. (The movie can be found in [79]) Although this growth mode may seem natural at first sight, it is rather surprising, since each nanomesh unit contains 169 B-atoms and 169 N-atoms. A more careful inspection of the images revealed the presence of a highly mobile species at the edges of the *h*-BN islands. We interpret this as BN diffusing along the island perimeter, until it locally accumulated into a new, complete nanomesh unit cell. At this point, the atoms in this nanomesh unit were effectively immobilized in their new structure.

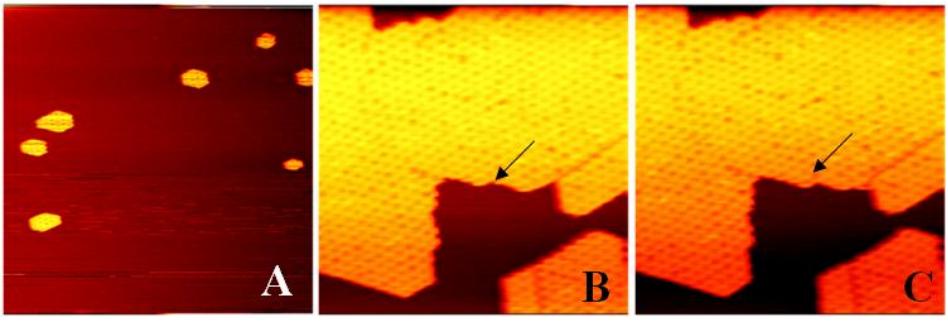

Fig. 4.3 (A) Rh(111) pre-seeded with nanomesh islands, by exposure to 0.2 L of borazine at room temperature, and subsequent annealing at 978 K. In this way, the nucleation density was artificially increased with respect to the natural density at 978 K. (B, C) Two subsequent STM images (17.5 s each) at 978 K during nanomesh growth on the pre-seeded surface at a borazine pressure of 3×10^{-9} mbar. As indicated by the arrow in (B) and (C), the growth unit here is one nanomesh unit.
Image size: (A) 170×170 nm^2, (B) and (C) 85×85 nm^2, Sample voltage: $V_b = 1.0$ V. Tunneling current $I_t = 0.05$ nA.

4.4.2 Nanomesh island shape

After the pre-seeded Rh sample had been annealed at 978 K (see previous section), the observed equilibrium island shape (Fig. 4.4A) was a quasi-hexagon, with three short and three long edges, corresponding to a higher-energy and a lower-energy termination of the island, respectively. The shape of the islands is the two-dimensional Wulff shape [81]. We associate the difference with the two different ways the edges can be terminated:

either with B atoms or with N atoms. In ref. [24], the lower-energy edge on Ni(111) was speculated to be N-terminated. The ratio E_L/E_H between the (free) energies of the two edges can be calculated from their length ratio to be 0.9 ± 0.1.

4.4.3 Nanomesh growth along different edges

When borazine was deposited, the island rapidly evolved into a (truncated) triangular growth shape (Fig. 4.4B). New nanomesh units formed naturally at kinks, which made these kinks advance along the island perimeter (Fig. 4.4). Although the kinks were found to advance with equal speeds along the two types of edges, the rates at which new kinks formed were different. The low-energy (longer) edges formed fewer kinks per unit length and time than the high-energy (shorter) edges. This is why the inequivalence between the two types of edges was emphasized by the growth, making the growth shape deviate even further from an equal-sided hexagon than the equilibrium shape from which the growth started. For a quantitative analysis we have used part of the seeding and growth experiments described in section 4.4.4. Images at the beginning and end of the analyzed episodes are shown in Fig. 4.6. Table 4.1 lists the kink creation rates measured for the short and the long edges of the island marked by the circle in panels A and B of Fig. 4.6. The table shows that the kink creation rates on the two types of edges differed by a factor of approximately 40, even though the bare Rh that surrounded this island was connected, so that the concentrations of BN experienced by all island edges must have been similar. The lower kink creation rate on the low-energy edge is easy to understand. The size of a complete nanomesh unit cell is so large, that the energy of a kink along a low-energy edge will be relatively close to the energy of one unit cell length of the high-energy edge (see the inset in Fig. 4.4C). Similarly, a kink along a high-energy edge will introduce an extra energy close to that for one unit cell length of the low-energy edge. The corresponding difference in kink energy will naturally make the kink creation rate lower on the low-energy edge.

On both types of edge, a kink can be regarded as a connection between a segment of high-energy and an equally long segment of low-energy edge. In view of this equivalence and of the fact that the energy is not changing with the position of the advancing kinks, we should expect the BN deposition to make existing kinks move equally fast along the two types of edges. Indeed, the measured rates at which kinks were observed to

advance along short and long edges were equal within the statistical error margin of the measurement, as shown in Table 4.1.

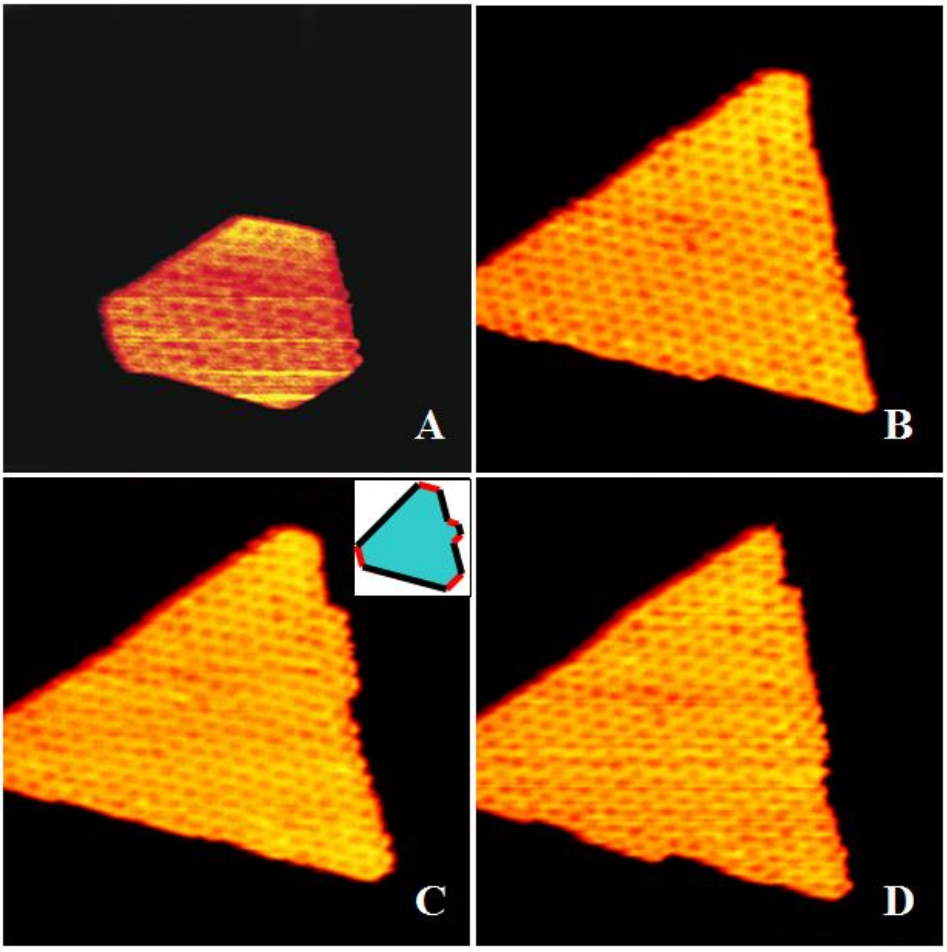

Fig. 4.4 STM images of an *h*-BN island, recorded at 978 K, while borazine was being deposited onto the Rh (111) surface; the images were selected from Movie 2 [79]. (A) The initial equilibrium island shape was obtained by exposing the clean Rh(111) surface to 0.2 L of borazine at room temperature, and subsequent annealing at 978 K. (B) Image after 368 s of borazine exposure at 2.5 $\times 10^{-9}$ mbar at 978 K; the island shape had become triangular, within the first 60 s. (C) After 421 s, new kinks had formed on the right edge, while the kink at the bottom edge had advanced to the right corner. The inset is a sketch, indicating the two types of edges, the red ones having the higher energy. (D) After 473 s, the two kinks on the right edge had advanced and new kinks had formed on the lower edge.

4.4.4 Growth barriers of the nanomesh structure at various sites

In this section, we use our STM movies to determine the growth rates of the nanomesh overlayer at various sites that play a special role in the growth process. The ratios between these rates allow us to determine the edge energies and corner energies of the *h*-BN structure.

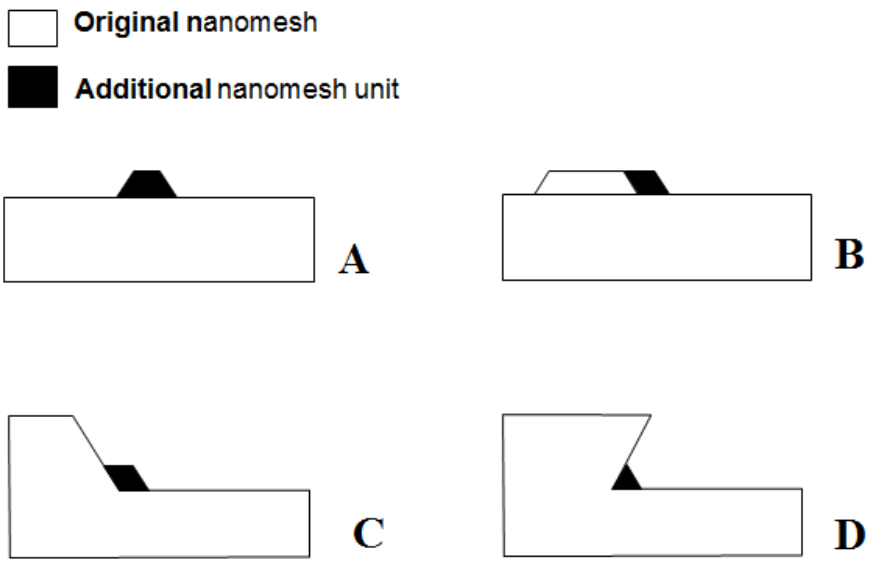

Fig. 4.5 Sketches of the essential steps in the growth of the nanomesh structure on different edge and corner sites. Note that the growth proceeds in complete unit cells of the nanomesh pattern. (A) Addition of the first unit cell of a new nanomesh row on a straight edge, involving the introduction of two kinks. This process costs less energy on high-energy edges, where the new unit introduces two additional low-energy edge segments. (B) advancement of an existing kink. The total edge energy remains unchanged in this process, so that it should have the same rate on low- and high-energy edges. (C) Addition of a nanomesh unit in 120 °corner. . This process differs from kink advancement, because two additional corners are created by this process. (D) Addition of a nanomesh unit in a 60 °corner.

In addition to the low- or high-energy straight edges (Fig. 4.5A, B), there are further sites from which the nanomesh structure can nucleate and grow. For example, Fig. 4.5C

sketches the filling of a 120° corner. Although this may look similar to the advancement of an existing kink (Fig. 4.5B), since no new edges are introduced, the nucleation in the corner does require the introduction of two extra corners, one concave and the other convex. This is reflected in the filling rate for 120° corners in Table 4.1, which is higher than the creation rate for new kinks on straight edges (both short and long), but lower than the rate at which kinks advance along straight edges. The filling rate for 120° corners was measured from the edges of the corner indicated by the circle in panels C and D of Fig. 4.6. These STM images were taken continuously, while the borazine pressure was kept at 3 x 10^{-9} mbar. The borazine pressures in the A-B and C-D series have been equal and also the kink advance rates measured in both series on the low-energy edges have been close to identical. This indicates that the BN concentrations have been similar for the two cases, which is why we can safely compare all rates from the two series in Table 4.1. Fig. 4.5D shows that the filling of a 60° corner replaces two low-energy sections by one high-energy section, provided that the edges of this corner are indeed low-energy edges. The measurement in Table 4.1 shows that this makes the filling rate for these corners somewhat lower than that for 120° corners. For completeness, we can also imagine a corner with two high-energy edges, but such a configuration would be filled very quickly, because two complete high-energy edges can then be replaced by one low-energy edge.

From the rates in Table 4.1, we can easily compute the differences in the activation barriers for the processes considered, according to the corresponding Boltzmann factors. For example, the ratio between two rates R_1 and R_2 provides us with the difference between the energy barriers E_1 and E_2 between processes 1 and 2, via $R_2/R_1 = e^{(E_1-E_2)/k_BT}$. Here, T is the temperature of the sample, k_B is Boltzmann's constant and we have assumed the pre-exponential factors for the two processes to be identical. We justify the latter assumption in two steps. First of all, the processes considered in Fig. 4.5 and Table 4.1 all proceed in the same units, namely the units of the nanomesh pattern. Secondly, in the experiments used for the rate measurements, the borazine pressure was constant, and the measured growth rates did not change significantly with time, showing that the surface concentration of BN has been constant and equal for the different edges and corners. Since we can only determine energy differences from the ratios between the rates, the energy barriers in Table 4.1 are all expressed relative to the energy barrier for the fastest process, namely the advancement of a kink along a low-energy (i.e. long) straight island edge.

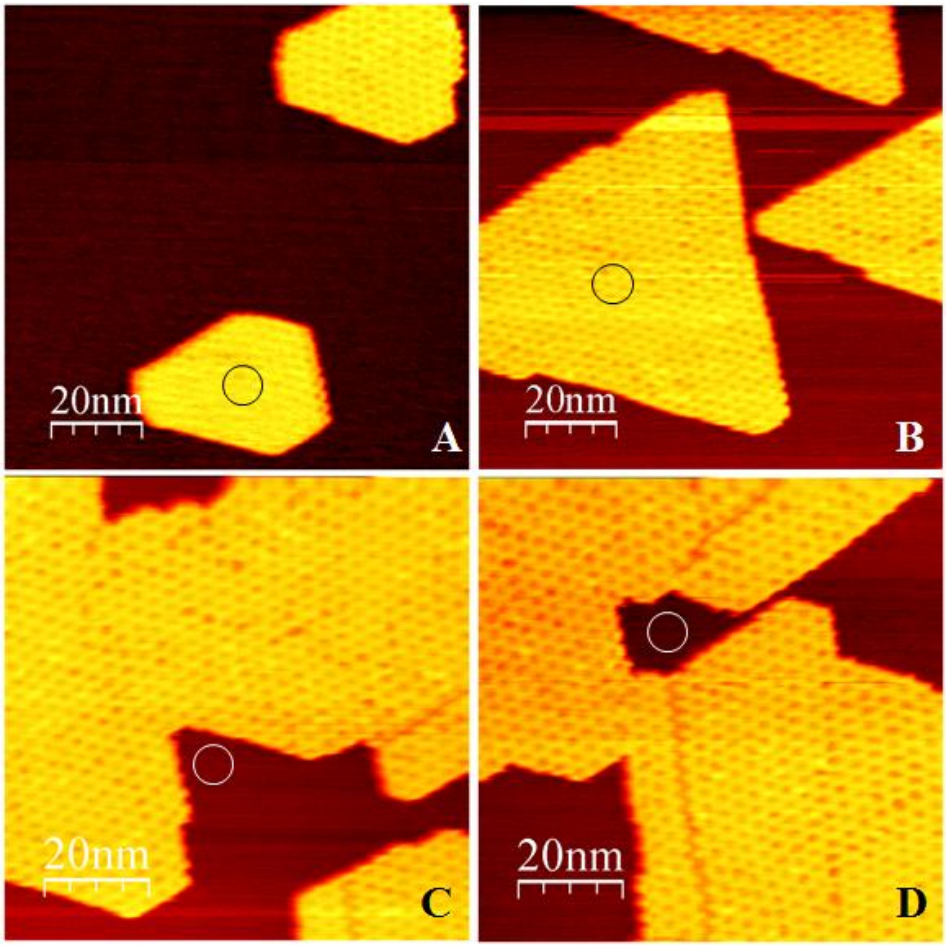

Fig. 4.6 First and last images in the two episodes (A-B and C-D) of an STM movie [79] of the high-temperature growth of the nanomesh structure on Rh(111) that have been used for the quantitative growth rate analysis. In A-B, the island marked by the circle was used. The Rh around the island was connected, so that the edges of the island were all exposed to the same densities of B and N atoms. In C-D, the growth rates of the edges around the circle were analyzed. The borazine pressure was 3 x 10^{-9} mbar and the sample was at 978 K.
Episode A-B was measured with 35 to 52.5 s per frame. Episode C-D with 17.5 s per frame. Image sizes were 100 × 100 nm^2 for A-B and 85 x 85 nm^2 for C-D. Sample voltage: V_b = 1.0 V. Tunneling current I_t = 0.05 nA.

	Rate (nanomesh units / site / second)	Relative energy barrier (eV)
Kink creation (short edges)	0.011 ± 0.002	0.15
Kink advancement (short edges)	0.058 ± 0.02	0.013
Kink creation (long edges)	0.00028 ± 0.00008	0.47
Kink advancement (long edges)	0.069 ± 0.008	0
120° corner filling	0.028 ± 0.005	0.077
60° corner filling*	0.019 ± 0.004	0.11

***** The data in the last line of the table were obtained on a 60 ° corner, accompanied by a domain boundary (see text)

Table 4.1 Rates of various basic processes involved in the growth of the nanomesh overlayer, measured at a borazine pressure of 3.0 x 10^{-9} mbar and at a temperature of 978 K. The margins reflect the statistical uncertainties. The energy barriers have been obtained from the rates using the procedure explained in the text and are expressed with respect to the energy barrier for the advancement of kinks along long (low-energy) edges.

The equality of the kink advancement rates of the different edge types shows that the corresponding activation energies have been equal to within statistical error, as expected (see above). The factor 40 difference in kink creation rate between the high- and low-energy edges shows, that the formation energy for a new kink is 0.32 eV higher on a low-energy edge than on a high-energy edge. Let us look in more detail at this difference. If we regard the edge of an *h*-BN island energetically as a straightforward sum of edge and corner energies, the energy involved in the addition of a 'single-nanomesh-unit' kink pair along a straight, low-energy island edge amounts to $2E_H - E_L + 2E_{-120} + 2E_{120} - 3E_{nm}/2 + \Delta E_{nm}^{kink-pair}$. In this expression, $E_L$and E_H are the (free) energies per unit length for the low- and the high-energy edges; for convenience we have expressed the length in units of the lattice constant of the nanomesh pattern. The energy change indicates that we are adding two kinks, i.e. two edge units of the high-energy orientation; but due to the 120° angles that these edge units make with the original edge, the total length of low-energy edge is reduced by one unit. E_{-120} and E_{120} are the corner energies for the two additional convex and the two additional concave 120° corners. E_{nm} is the amount by which the total (free) energy is lowered by the incorporation of 169 B and 169 N atoms in a unit cell of the *h*-BN structure. The factor $3/2$ appears because the shape defined by

the two high-energy edges and one unit of the low-energy edge is actually $3/2$ times the size of a single nanomesh unit. Finally, $\Delta E_{nm}^{kink-pair}$ is the (free) energy barrier associated with the accumulation of the 211 B atoms and 211 N atoms in this initial kink pair structure. On the high-energy edge, the corresponding energy is to $2E_L - E_H + 2E_{-120} + 2E_{120} - 3E_{nm}/2 + \Delta E_{nm}^{kink-pair}$. We see that in this description, the difference in energy barrier can be related directly to the difference in formation energy of high- and low-energy edges: $3(E_H - E_L) = 0.32$ eV. Since we also know the ratio between these energies from the equilibrium shape (see above), we can now calculate the two energies to be $E_H = 1.1$ eV and $E_L = 0.96$ eV. Even though these are crude estimates, in view of the combination of the error margins on the energy difference and on the energy ratio, it is clear that the edge free energies of the *h*-BN overlayer on Rh(111) are rather low, certainly if we realize that these energies are expressed per unit of length of the nanomesh pattern; per unit cell length of the overlayer itself, the edge energies are as small as 82 meV and 74 meV. For 120° corner filling, the activation energy is expected to be $E_{-120} + E_{120} - E_{nm} + \Delta E_{nm}^{120^\circ}$. The fact that the observed rate for the filling of 120° corners is lower than the kink advancement rate, which should have an activation energy of $-E_{nm} + \Delta E_{nm}^{\mathrm{kink-adv}}$, where we expect the two activation energies, $\Delta E_{nm}^{120^\circ}$ and $\Delta E_{nm}^{\mathrm{kink-adv}}$, to be close to identical, shows that $E_{-120} + E_{120}$ is nonzero and positive. We find $E_{-120} + E_{120} = 76$ meV, which shows that the corner energy is of the same order of magnitude as the edge energy of a single lattice spacing of the *h*-BN overlayer. We estimate that the energy associated with the filling up of a 60° corner is actually negative. This should make the rate of filling up of such corners very high. Indeed, we have not observed such corners in our movies, except in cases, where they were accompanied by a defect, such as the domain boundary, clearly visible at the 60° corner that is partly filled up in Fig. 4.6D.

4.5 Conclusions

In this chapter we have investigated the growth of *h*-BN from borazine deposited on Rh(111) at various temperatures. Deposition at room temperature and at 627 K did not yet lead to the formation of *h*-BN. Instead, higher-temperature deposition, e.g. at 865 K, or higher-temperature annealing after low-temperature deposition was required to form

h-BN. The borazine was concluded to start decomposing at a temperature between 762 and 806 K.

Borazine deposition at high temperatures, close to the reported optimal conditions, e.g. at 978 K, was found to lead to nanomesh patches that were well-aligned with the Rh(111) substrate. To our surprise, we observed a large growth unit of the overlayer of a full period of the nanomesh superstructure, which contains as much as 169 BN units.

After initial nucleation, the growth of the *h*-BN nanomesh structure can be separated into two steps: creation of new kinks and advancement of existing kinks. The kink creation rate is different for B-terminated and N-terminated edges, while the advancement rate is similar for both. This is explained by comparing the local structures of the kinks on these edges. From the observed growth rates and equilibrium shapes we have determined that the edge energies are 82 and 74 meV per BN lattice unit for the high- and low-energy edges, respectively, and that the sum of the energies for a 120º and a -120º corner is 76 meV.